第 31 卷第 10 期
2015 年 10 月

无 机 化 学 学 报
CHINESE JOURNAL OF INORGANIC CHEMISTRY

Vol.31 No.10
2073-2078

基于半刚性四面体四齿配体构筑的 Zn(Ⅱ)/Cd(Ⅱ)配位聚合物及其性质

唐文渊[1] 任世斌*,[1,2] 朱冬冬[1] 韩得满[1] 周馨慧*,[3]

([1]台州学院医药化工学院,台州 317000)

([2]南京大学化学化工学院生命分析化学国家重点实验室,南京 210093)

([3]南京邮电大学有机电子与信息显示国家重点实验室及先进材料研究所,南京 210023)

摘要:在水热的条件下,利用四(4-吡啶氧甲基)甲烷(L_1)或四(3-吡啶氧甲基)甲烷(L_2)、1,4-萘二甲酸(1,4-NDC)和 d^{10} 金属离子发生自组装反应合成了 2 个化合物$\{[Cd_2(L_1)(1,4\text{-NDC})_2]\cdot 2H_2O\}_n$ (**1**)和$\{[Zn_2(L_2)(1,4\text{-NDC})_2]\cdot DMF\cdot 3H_2O)\}_n$ (**2**)。单晶结构表明化合物 **1** 是通过 L_1 配体与一维链$[Cd(1,4\text{-NDC})]_n$ 相连构建而成的三维骨架化合物,而化合物 **2** 是一对螺旋链与另外的一维链相互垂直交联而形成二维网络结构。更为重要的是,通过引入 2 种不同空间位阻的配体,研究了辅助配体对金属有机配位聚合物结构多样性的影响。另外,它们的荧光性质也做了相应的探讨。

关键词:羧酸配体;异构化;空间位阻;荧光

中图分类号:O614.24+2;O614.24+1 **文献标识码**:A **文章编号**:1001-4861(2015)10-2073-06

DOI:10.11862/CJIC.2015.229

Crystal Structures and Properties of Zn(Ⅱ)/Cd(Ⅱ) Coordination Polymers Based on Semirigid Tetrahedral Quadridentate Ligand

TANG Wen-Yuan[1] REN Shi-Bin*,[1,2] ZHU Dong-Dong[1] HAN De-Man[1] ZHOU Xin-Hui*,[3]

([1]*School of Pharmaceutical and Chemical Engineering, Taizhou University, Taizhou, Zhejiang* 317000, *China*)

([2]*State Key Laboratory of Analytical Chemistry for Life Science, School of Chemistry and Chemical Engineering, Nanjing University, Nanjing* 210093, *China*)

([3]*Key Laboratory for Organic Electronics & Information Displays (KLOEID) and Institute of Advanced Materials (IAM), Nanjing University of Posts & Telecommunications, Nanjing* 210023, *China*)

Abstract: Two complexes, $\{[Cd_2(L_1)(1,4\text{-NDC})_2]\cdot 2H_2O\}_n$ (**1**) and $\{[Zn_2(L_2)(1,4\text{-NDC})_2]\cdot DMF\cdot 3H_2O)\}_n$ (**2**) (L_1=tetrakis(4-pyridyloxymethylene)methane, L_2=tetrakis(3-pyridyloxymethylene)methane, 1,4-NDC=naphthalene-1,4-dicarboxylic acid) are obtained by the self-assembly reaction of L_1 or L_2, 1,4-NDC, and d^{10} metal ions under solvothermal conditions. The X-ray analysis reveals that **1** is constructed from a 1D zigzag chain $[Cd(1,4\text{-NDC})]_n$ which is linked by L_1 ligand to yield a 3D framework. And yet in case of **2**, one double helix is mutually interdigitated by another 1D chain into a 2D network. Above all, the effect of steric hindrance of the auxiliary linker on the structural diversity of CPs can be discussed in great detail by the introduction of two kinds of auxiliary linkers with different steric hindrance. Additionally, their luminescent properties are also observed. CCDC: 1019510, **1**; 1019511, **2**.

Key words: carboxylate ligands; isomerization; steric hindrance; luminescence

收稿日期:2015-04-13。收修改稿日期:2015-05-14。

国家自然科学基金(No.21471110,21375092),浙江省自然科学基金(No.LY12B01006),中国博士后基金(No.2013M531314),生命分析国家重点实验室开放课题(No.SKLACLS1206),浙江省大学生创新计划项目(No.2014R428014),台州市科技局项目(No.131KY03)及浙江省科技厅公益分析测试项目(No.2015C37034)资助项目。

*通讯联系人。E-mail:renshibin@tzc.edu.cn; iamxhzhou@njupt.edu.cn;会员登记号:S06N4804M1203。

The study of coordination polymers (CPs) has received increasing interest owing to their fascinating architectures and topologies as well as many potential applications[1]. The unique properties of CPs are closely related to their specific structures. In the context, the rational selection of metal ions and linker geometries are of great importance in controlling their desired architectures and functionalities[2]. In particular, auxiliary linkers also play a marvelous role in the construction of CPs. Auxiliary aromatic carboxylates have great influence on the structural diversity by the post-synthetic modification or the change of the position and amounts of carboxylic groups[3]. However, the systematic study on structural change of CPs helps us to predict and synthesize coordination polymers with expected structures, which enable us to well-tune the structure and function of CPs.

To a large extent, the structural diversity mainly depends on organic linkers, which offers the opportunity to functionalize porous frameworks. In recent years, a large number of studies have been reported that the CPs built from mixed ligands, especially from N-donor ligands and aromatic carboxylate, will exhibit more diverse and fascinating networks with potential applications[4]. Additionally, it is well known that using mixed linkers will become more easy for the targeted synthesis of CPs than using a single ligand[5]. However, as far as we know, the study on the effect of steric hindrance of an auxiliary linker on the structural diversity of CPs remains largely unexplored.

The incorporation of mixed linkers within CPs offers a significant opportunity to explore the influence factor of their structural change. Herein, we have chosen a couple of N-donor linkers, tetrakis(4-pyridyloxymethylene)methane (L_1) and tetrakis(3-pyridyloxymethylene)methane(L_2), due to their specific configurations and flexible conformers[4,6]. Additionally, naphthalene-1,4-dicarboxylic acid (1,4-NDC) is used as an auxiliary linker to explore the effect of steric hindrance on structural diversity of CPs. We have prepared two complexes: one non-interpenetration network and another threefold interpenetration network, which are built from L_1 and L_2, respectively[4a,6c]. Herein, two complexes based on d^{10} metal ions, L_1 or L_2 and 1,4-NDC have been successfully prepared under hydrothermal conditions (Scheme 1). They are also characterized by X-ray crystallography, elemental analysis, infrared spectra (IR), powder X-ray diffraction (PXRD), and thermogravimetric (TG) analyses. Besides, photoluminescence and the effect of steric hindrance of an auxiliary linker on the structural diversity of CPs have been discussed.

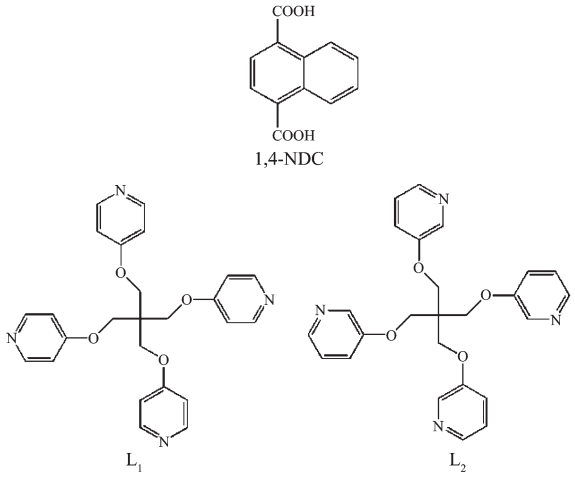

Scheme 1 Structure of organic ligands

1 Experimental

1.1 Materials and methods

Ligand L_1 and L_2 was prepared according to the literature[6d]. Reagents and solvents employed were commercially available. The C, H, and N microanalyses were carried out with a Perkin-Elmer PE 2400 Ⅱ CHN elemental analyzer. Fourier transform infrared (FT-IR) spectra of the compounds were obtained in the 4 000~400 cm^{-1} region on a Bruker Vector 22 spectrophotometer with KBr pellets. Powder X-ray diffraction (PXRD) measurements were obtained on a Bruker D8 Advance X-ray diffractometer with Cu $K\alpha$ radiation. Thermal analyses (TG) were performed in a nitrogen stream using Seiko Extar 6000 TG equipment with a heating rate of 10 ℃·min^{-1}. Luminescence spectra were recorded on a Hitachi 850 fluorescence spectrophotometer.

1.2 Synthesis of complexes

1.2.1 Synthesis of $\{[Cd_2(L_1)(1,4\text{-NDC})_2]\cdot 2H_2O\}_n$ (**1**)

A mixture of L_1 (0.044 4 g, 0.1 mmol), 1,4-NDC

(0.021 6 g, 0.1 mmol) and $Cd(NO_3)_2\cdot 4H_2O$ (0.061 7 g, 0.20 mmol) in CH_3CN and H_2O (1∶1, *V*/*V*) was sealed into a 30 mL Teflon lined stainless steel vessel and heated to 90 ℃ for 3 days. After the mixture was cooled to room temperature, brown rodlike crystals of **1** suitable for X-ray diffraction analyses were obtained in the yield of 25.7%. Elemental analysis Calcd. for $C_{49}H_{40}Cd_2N_4O_{14}$(%): C, 51.9; H, 3.6; N, 4.9. Found(%): C, 5.20; H, 3.7; N, 4.8. Selected IR data (KBr, cm^{-1}): 3 250 (m), 2 427(w), 1 685 (s), 1 600(m), 1 559(s), 1 536(w), 1 398(s), 1 356(m), 1 327(m), 1 294(m), 1 258(w), 1 194(w), 933(w), 795(s).

1.2.2　Synthesis of $\{[Zn_2(L_2)(1,4\text{-NDC})_2]\cdot DMF\cdot 3H_2O)\}_n$ (**2**)

A mixture of L_2 (0.044 6 g, 0.1 mmol), 1,4-NDC (0.021 6 g, 0.1 mmol) and $Zn(NO_3)_2\cdot 6H_2O$ (0.059 5 g, 0.20 mmol) in DMF and H_2O (1∶1, *V*/*V*) was sealed into a 30 mL Teflon lined stainless steel vessel and heated to 90 ℃ for 3 days. After the mixture was cooled to room temperature, yellow block crystals of **2** suitable for X-ray diffraction analyses were obtained in the yield of 35.2%. Elemental analysis Calcd. for $C_{52}H_{49}N_5O_{16}Zn_2$ (%): C, 55.2; H, 4.4; N, 6.2. Found (%): C, 55.1; H, 4.5; N, 6.1. Selected IR data (KBr, cm^{-1}): 3 152(m), 1 650(m), 1 500(m), 1 411(s), 1 400 (s), 1 359(s), 1 194(m), 1 103(m), 929(m), 788(w).

1.3　X-ray crystallography

The single-crystal X-ray data collection for **1** and **2** was performed on a Bruker SMART APEX CCD diffractometer with graphite-monochromated Mo *Kα* radiation (*λ*=0.071 073 nm) at room temperature. Data reductions and absorption corrections were performed using the SAINT and SADABS software packages, respectively. Raw frame data were integrated with the SAINT program[7a]. The structure was solved by direct methods and refined by full-matrix least-squares on F^2 using SHELX-97[7b]. An empirical absorption correction was applied with the program SADABS[7c]. All non-hydrogen atoms were refined anisotropically. Hydrogen atoms were set in calculated positions and refined by a riding mode, with a common thermal parameter. The relevant crystallographic data are presented and selected bond lengths and angles are given in Table S1~2.

CCDC: 1019510, **1**; 1019511, **2**.

2　Results and discussion

2.1　Descriptions of crystal structures

2.1.1　Crystal structure of $\{[Cd_2(L_1)(1,4\text{-NDC})_2]\cdot 2H_2O\}_n$ (**1**)

The crystal structure determination reveals that **1** crystallizes in the orthorhombic system and space group Pnnm. The asymmetric unit contains one Cd atom, a half of L_1, one deprotonated 1,4-NDC and one coordinated water molecule. Each Cd atom coordinates to three oxygen atoms from two distinct 1,4-NDC and two nitrogen atoms from two distinct L_1 (Fig.1a). The rest of the coordination sites in each Cd atom are occupied by one water molecule. Thus, each Cd atom has adopted a distorted octahedral geometry. Cd-O and Cd-N distances lie in the ranges of 0.225 0 (3)~0.237 8(2) nm and 0.229 4(3)~0.230 0(3) nm, respectively, and the corresponding bond angles around each Cd atom are in the range of 27.50(12)°~169.26(12)°. Each couple of L_1 shares two Cd atoms through its N-donors to form infinite chains parallel to each other. On the other hand, 1,4-NDC adopts μ_2-η^1:η^1 or μ_2-η^2:η^2-fashion alternatively to connect Cd atoms via its

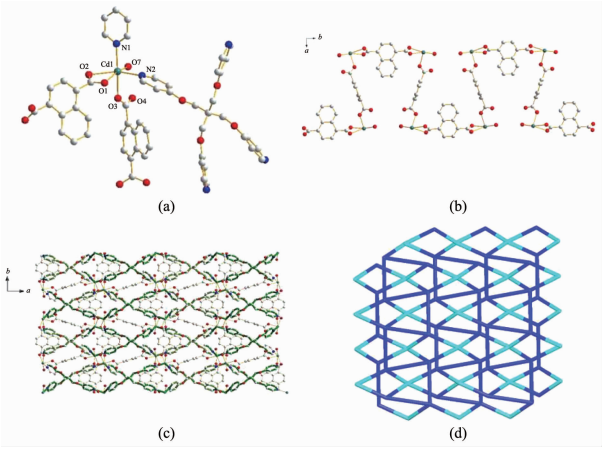

Hydrogen atoms and free water molecules are omitted for clarity in (a)

Fig.1　(a) Coordination environments of Cd atoms in **1**; (b) 1D zigzag chain formed by Cd-1,4-NDC; (c) 3D structure formed by the coordination of pyridyl N-donors of L_1 with Cd atoms in 2D chain; (d) Schematic view of the topological structure of **1**

carboxylate groups, resulting in a 1D zigzag chain $[Cd(1,4\text{-NDC})]_n$ (Fig.1b). The 1D chain $[Cd(1,4\text{-NDC})]_n$ is threaded with L_1 ligand via sharing the metal sites to yield a 3D framework (Fig.1c). Topologically, if L_1 and Cd atoms are viewed as (4,4)-connected nodes, respectively, the overall motif of **1** is a 2-nodal (4,4)-connected $(5\cdot6^2\cdot7^2\cdot8)(5^2\cdot6\cdot7\cdot8^2)_2$ network (Fig.1d).

2.1.2 Crystal structure of $\{[Zn_2(L_2)(1,4\text{-NDC})_2]\cdot DMF\cdot 3H_2O)\}_n$ (**2**)

Complex **2** crystallizes in the monoclinic system with the $P2_1/n$ space group. The single-crystal X-ray analysis of **2** revealed one Zn(Ⅱ) atom, one L_2, two deprotonated 1,4-NDC, a lattice DMF and three free water molecules in the asymmetric unit. As shown in Fig.2a, each Zn atom is pent-coordinated by two nitrogen atoms from two L_2 and three oxygen atoms from two 1,4-NDC. The Zn-N and Zn-O bond distances are in range of 0.203 4(3)~0.208 7(3) nm and 0.193 8(3) ~0.198 2(3) nm, respectively. The bond angles around the Zn atom vary from 94.47(12)° to 132.31(13)°, adopting the trigonal bipyramid geometry. Each L_2 acts as a tetradentate bridging ligand and joins four Zn atoms to form a 1D chain. Additionally, adjacent two 1,4-NDC are joined end to end by sharing Zn atoms to produce an arched chain, weak interactions between which accelerate the formation of an unprecedented double helix (Fig.2b). As a result, these helix are extended by L_2 to afford a 2D sheet (Fig.2c). From a topological point of view, the central Zn atom and L_2 ligand are viewed as 4-connecting nodes, respectively, the overall motif of **2** is a 2-nodal (4,4)-connected $(4\cdot6^4\cdot7)^2(4^2\cdot6^2\cdot7\cdot8)$ net (Fig.2d).

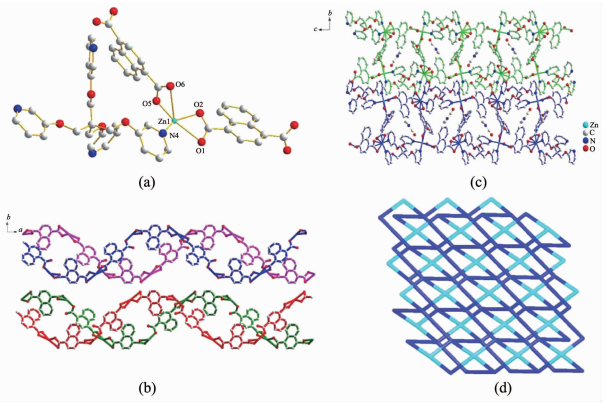

Fig.2 (a) Coordination environment of Zn atoms in **2**; (b) 1D chain in **2**; (c) 2D layer of **2**; (d) Schematic 2-nodal (4,4)-connected $(4\cdot6^4\cdot7)^2(4^2\cdot6^2\cdot7\cdot8)$ net in **2**

2.2 Effect of steric hindrance of an auxiliary linker on the structural diversity

We tried to explore the effect of steric hindrance of an auxiliary linker on the structural diversity of CPs. The phenomenon can be explained by the introduction of an couple of 1,4-BDC and 1,4-NDC within the study system. For **1** and Ⅰ, the change of the auxiliary linker will bring about the variation of coordination modes, which vary from μ_2-η^1:η^1-fashion to μ_2-η^1:η^1 and μ_2-η^2:η^2-fashion. The change of the auxiliary linker from 1,4-NDC to 1,4-BDC result in the change of their topology from 2-nodal (4,4)-connected $(5\cdot6^2\cdot7^2\cdot8)(5^2\cdot6\cdot7\cdot8^2)_2$ network to 2-nodal (4,4) -connected $(6^2\cdot8^4)$ network (**1** and Ⅰ in Fig.3). In contrast, for **2** and Ⅱ, they exhibit a 3D network and 2D layer structure, respectively. But it is worth nothing that the change of the auxiliary linker enable their structures to vary from 2-nodal (4,4)-connected $(4\cdot6^4\cdot7)^2$ $(4^2\cdot6^2\cdot7\cdot8)$ net to 3-nodal (4,6)-connected $(3\cdot4\cdot5^2\cdot6^2)(3^4,4^2,5^3\cdot6^5\cdot7)_2(4\cdot5^2\cdot6^2\cdot7)$ net (**2** and Ⅱ in Fig.3). As far as their component are concerned, the structure of **1** and I both contain the same componentsthe central d^{10} ions and L_1 except for auxiliary linker. As a matter of fact, the difference in their structure is attributed to the significant steric hindrance of 1,4-NDC over those of BDC. Therefore, topological structure of **1** and **2** is a far cry from that of their

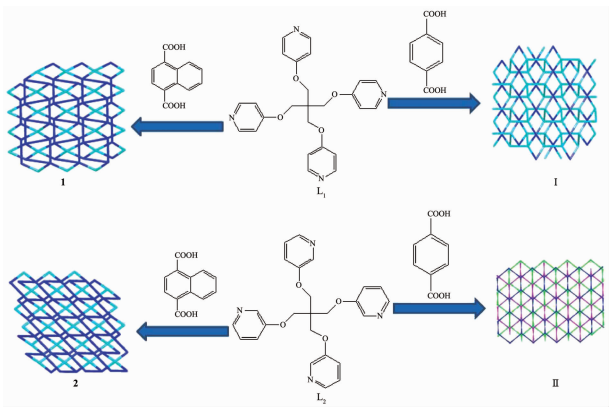

Fig.3 Schematic view of control over the structural diversity by adjusting the steric hindrance of an auxiliary linker

counterparts Ⅰ and Ⅱ on account of distinct steric hindrance of auxiliary linkers. In conclusion, the effect of steric hindrance of an auxiliary linker will strongly affect the structural diversity of CPs.

2.3 X-ray powder diffraction and thermal analyses

To confirm whether the single crystal structure is truly representative of the bulk materials, powder X-ray diffraction measures were carried out for **1** and **2** at room temperature. As shown in Fig.S1, the peak positions of the experimental and simulated XRPD patterns are in agreement with each other, suggesting the presence of the phase purity in the corresponding samples **1** and **2**. Thermal gravimetric analysis was performed for **1** and **2** under N_2 atmosphere with a heating rate of 10 ℃·min^{-1} in the temperature range of 25~800 ℃ (Fig.S2). The TGA curve of **1** shows a weight loss of 6.2% (Calcd. 3.2%) from room temperature to 187 ℃ corresponding to the release of the surface and included water molecules and then there is an intense weight loss from 491.8 ℃, which is attributed to the decomposition of the framework. For **2**, the weight loss of 3.5% (Calcd. 3.1%) attributed to the gradual release of the surface and included water molecules is observed in the range of 20.1~220.5 ℃, the framework retains in the temperature range of 220.5~491.8 ℃, and then decomposes.

2.4 Photoluminescence

Coordination complexes with d^{10} metal ions have been investigated for luminescent properties as well as their potential applications in electroluminescent displays, chemical sensors, and photochemistry[8]. The changeable luminescent features are originated from adopting different coordination modes around d^{10} metal ions, interaction with bridging linkers, and so on. The solid state luminescent properties of free L_1, L_2, **1** and **2** were studied at room temperature, as shown in Fig. 4. The ligand L_1 or L_2 displays obvious luminescent intensity in the range of 400~600 nm under excitation at 370 nm at room temperature. The emission spectra for **1** and **2** exhibit similar emission peaks at 417 nm. However, the relatively different intensities of the two emissions could result from the variety of coordinating modes of the metal ion with the bridging linker. Additionally, in view of the structural characteristic of d^{10} metal ion, the luminescent properties of **1** and **2** can be attributed to the mixture of ligand-centered emission and LMCT.

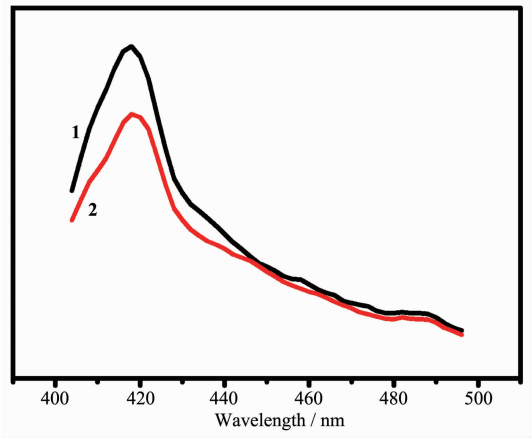

Fig.4　Solid-state luminescent spectra of **1** and **2**

3 Conclusions

In summary, we established an experimental diagram to study the effect of the steric hindrance of an auxiliary linker on the structural diversity of CPs by the incorporation of two kinds of auxiliary linkers with different steric hindrance into experimental systems. The relationship between the structural diversity of CPs and steric hindrance of the auxiliary linker can be well illustrated by comparing the topological structure **1** and **2** with those of Ⅰ and Ⅱ. In particular, L_1 or L_2 is appropriate for constructing various MOFs due to its specific tetrahedral configuration and flexible conformation. All this will provide us a research way to explore the structure-properties correlation for other similar systems.

Supporting information is available at http://www.wjhxxb.cn

References:

[1] (a)Moulton B, Zaworotko M J. *Chem. Rev.*, **2001**,**101**:1629-1658
(b)James S L. *Chem. Soc. Rev*., **2003**,**32**:276-288
(c)Ockwig N W, Delgado-Friedrichs O, O′Keeffe M, et al. *Acc. Chem. Res.*, **2005**,**38**:176-182
(d)Noro S, Kitagawa S, Kondo M, et al. *Angew. Chem. Int.*

Ed., **2000**,**39**:2081-2084

(e)Zhang J P, Lin Y Y, Huang X C, et al. *J. Am. Chem. Soc.*, **2005**,**127**:5495-5506

(f)Song X Z, Song S Y, Zhao S N, et al. *Adv. Funct. Mater.*, **2014**,**24**:4034-4041

[2] (a)Perry J J 4th, Perman J A, Zaworotko M J, et al. *Chem. Soc. Rev.*, **2009**,**38**:1400-1417

(b)Li J R, Sculley J, Zhou H C. *Chem. Rev.*, **2012**,**112**:869-932

(c)Farha O K, Hupp J T. *Acc. Chem. Res.*, **2010**,**43**:1166-1175

[3] (a)Ma T, Li M X, Wang Z X, et al. *Cryst. Growth Des.*, **2014**, **14**:4155-4165

(b)Zhang X, Hou L, Liu B, et al. *Cryst. Growth Des.*, **2013**, **13**:3177-3187

(c)Hua J A, Zhao Y, Liu Q, et al. *CrystEngComm*, **2014**,**16**: 7536-7546

(d)Lu X, Ye J, Li W, et al. *CrystEngComm*, **2012**,**14**:1337-1344

[4] (a)Ren S B, Zhou L, Zhang J, et al. *CrystEngComm*, **2010**, **12**:1635-1638

(b)Ren S B, Chen F J, Wu C L, et al. *J. Mol. Struct.*, **2013**, **1034**:193-197

(c)Ren S B, Qiu Z J, Yan J, et al. *J. Mol. Struct.*, **2013**,**1046**: 15-20

[5] (a)Paz F A A, Klinowski J, Vilela S M F, et al. *Chem. Soc. Rev.*, **2012**,**41**:1088-1110

(b)Liang X, Zhang F, Zhao H, et al. *Chem. Commun.*, **2014**, **50**:6513-6516

(c)Zhou X H, Li L, Li H H, et al. *Dalton Trans.*, **2013**,**42**: 12403-12409

[6] (a)Ren S B, Zhou L, Zhang J, et al. *CrystEngComm*, **2009**,**11**: 1834-1836

(b)Ren S B, Zhou L, Zhang J, et al. *Inorg. Chem., Commun.*, **2011**,**14**:558-561

(c)Ren S B, Lin Y Q, Zhang Q, et al. *Polyhedron*, **2014**,**83**: 130-136

(d)Zhang Q, Bu X, Lin Z, et al. *Inorg. Chem.*, **2008**,**47**:9724-9726

[7] (a)*SAINT-Plus, Version* 6.02, Bruker Analytical X-ray System, Madison, WI, **1999**.

(b)Sheldrick G M. *SADABS, An Empirical Absorption Correction Program*, Bruker Analytical X-ray Systems, Madison, WI, **1996**.

(c)Sheldrick G M. *Acta Crystallogr.*, **2008**,**A64**:112

[8] (a)He K H, Song W C, Li Y W, et al. *Cryst. Growth Des.*, **2012**,**12**:1064-1068

(b)Ren S B, Yang X L, Zhang J, et al. *CrystEngComm*, **2009**,**11**:246-248

(c)Lu Y B, Jian F M, Jin S, et al. *Cryst. Growth Des.*, **2014**, **14**:1684-1694